THERMAL PERFORMANCE OF A ROOF INTEGRATED SOLAR MICRO-CONCENTRATING COLLECTOR

Tanzeen Sultana[1], Graham L Morrison[1] and Gary Rosengarten[1]

[1] School of Mechanical and Manufacturing Engineering, University of New South Wales,

Sydney, NSW 2052, Australia

ABSTRACT

Concentrating solar thermal systems offer a promising method for large scale solar energy collection. Although concentrating collectors are generally thought of as large-scale stand-alone systems, there is a huge opportunity to use novel concentrating solar thermal systems for rooftop applications such as domestic hot water, industrial process heat and solar air conditioning for commercial, industrial and institutional buildings. This paper describes the thermal performance of a new low-cost solar thermal micro-concentrating collector (MCT), which uses linear Fresnel reflectors, and is designed to operate at temperatures up to 220°C. The modules of this collector system are approximately 3 meters long by 1 meter wide and 0.3 meters high. The objective of the study is to optimize the design to maximise the overall thermal efficiency. The absorber is contained in a sealed enclosure to minimise convective losses. The main heat losses are due to natural convection inside the enclosure and radiation heat transfer from the absorber tube. In this paper we present the results of a computational investigation of radiation and convection heat transfer in order to understand the heat loss mechanisms. A computational model for the prototype collector has been developed using ANSYS-CFX, a commercial computational fluid dynamics software package. The numerical results are compared to experimental measurements of the heat loss from the absorber, and flow visualization within the cavity. The efficiency of the collector is established on the basis of ray tracing and heat loss analysis.

1. Introduction

Concentrating solar collectors offer a promising method for large scale solar energy collection. It is feasible to use concentrating solar collectors for applications such as domestic hot water and industrial and institutional process heat. In recent years, many non-concentrating roof-integrated collectors have been proposed, such as hybrid systems with photovoltaic or thermoelectric elements (Juanico, 2008). Rooftop integrated concentrating solar thermal systems are not common, and only a few projects are mentioned in the literature (Gee et al., 2003, Petrakis et al. 2009, Sultana et al. 2010, 2011). Until now, the commercially available high temperature solar thermal technologies such as parabolic trough and linear Fresnel concentrators, have not integrated well on rooftops as they have been complex, cumbersome, have high wind loading and are difficult to maintain.

In this paper, a new low-cost micro-concentrator collector (MCT) has been studied, which is designed to operate at temperatures up to 220°C, and be seamlessly integrated into the architecture of buildings. The applications of this system include domestic hot water, industrial process heat and solar air conditioning for commercial, industrial and institutional buildings.

Rooftop collectors for solar cooling applications need to be very space efficient and be able to deliver energy above 140^{o}C as low temperatures can only be used to drive single effect chillers. Traditional flat plate solar collectors need more than twice the roof area to produce sufficient cooling for a low rise building. High temperature systems, such as parabolic trough collectors, require more space on the rooftop to avoid shading as they track the sun. In this regard the MCT is more efficient compared to both low temperature collectors and more complex high temperature systems (Sultana et at. 2010).

2. Overview of the MCT collector

The MCT system module is approximately 3.2 meters long by 1.2 meters wide and 0.3 meters high (Fig. 1). The MCT collector utilizes linear Fresnel reflector optics that concentrate beam radiation to a stationary receiver. The receiver consists of two 16 mm diameter stainless steel absorber tubes. Each receiver has a secondary reflector that directs beam radiation to the absorber tube. The entire optic system is enclosed in a sealed glazed canopy. The design of the receiver is illustrated in Fig. 2.

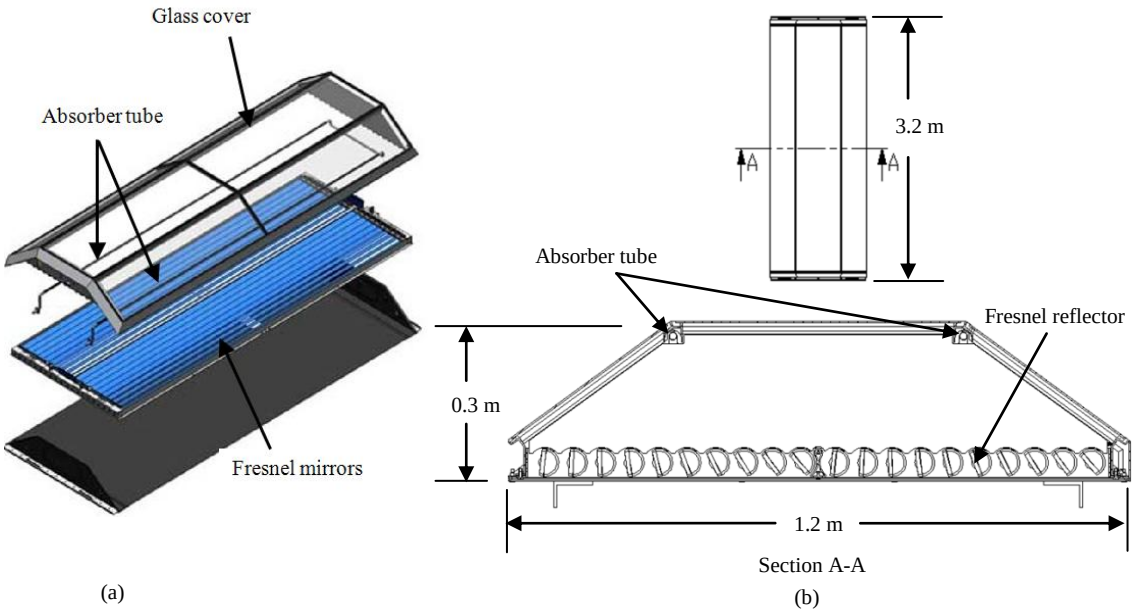

Fig. 1: (a) Exploded view of a solar micro-concentrator system (Chromasun, Inc.), (b) Cross-section of the MCT collector

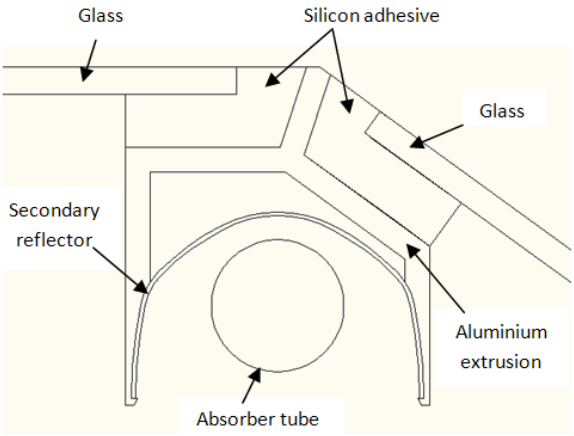

Fig. 2: Receiver design in the micro-concentrating collector

3. Heat Loss of MCT Collector

Evaluation of heat losses from the receiver is an important input to the performance evaluation of the solar collector. To achieve high efficiency in a concentrating solar collector, there should be minimum thermal losses from the absorber. Fig. 3 shows a schematic cross section of the collector along with the internal modes of heat transfer. During operation, the hot absorber tube emits long-wavelength radiation into the cavity that is absorbed mainly by the bottom wall, which in turn heats up. This promotes buoyancy-driven flows within the cavity, resulting in convection losses and a further reduction in thermal efficiency (Reynolds, 2004, Sultana et al. 2010).

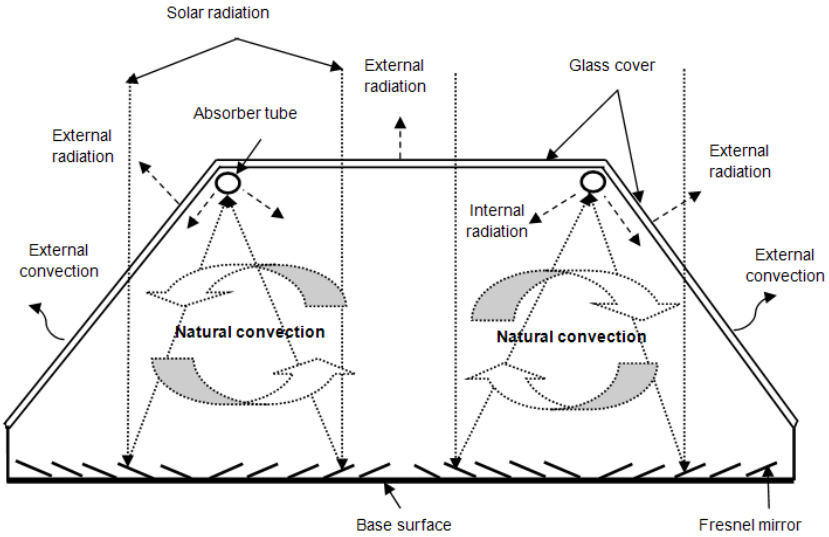

Fig. 3: Cross-section of the micro-concentrating collector showing modes of internal heat transfer

The current study investigates the role of radiation and natural convection heat transfer inside the cavity, along with heat transfer at the boundaries in order to fully understand the heat loss mechanisms.

4. Computational Modelling

A computational model of the prototype absorber has been developed using ANSYS-CFX (ANSYS, 2010). For simplicity, a two dimensional geometry with a symmetry plane is created (Fig. 4) assuming the collector is mounted flat on a roof.

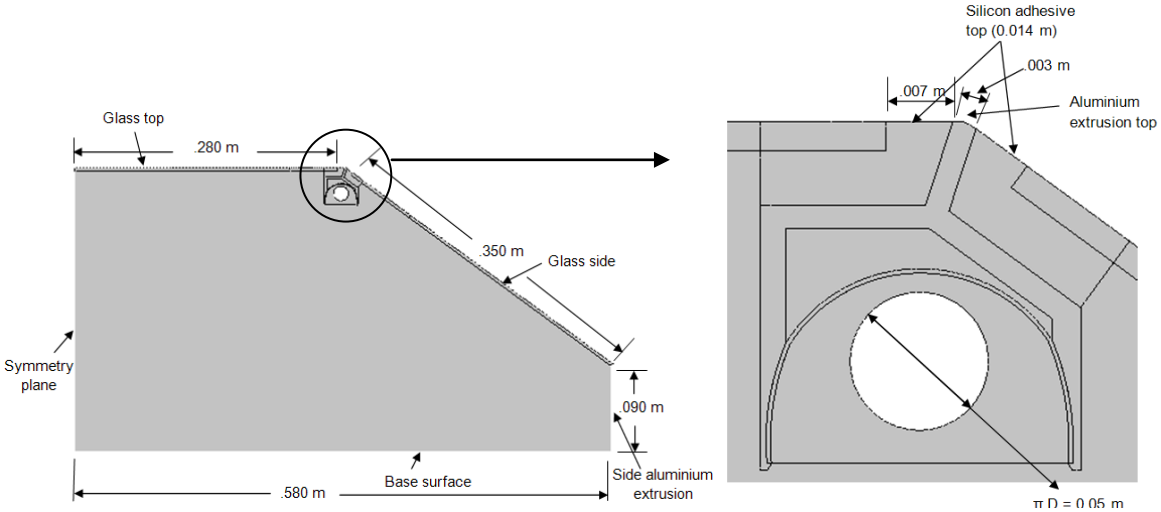

Fig .4: Cavity geometry for CFD modelling with zoomed up view of the receiver section (right)

The absorber tube is modelled as an isothermal surface. The convective flow and resulting temperature difference between the absorber tube and the secondary reflector and glass cover are studied for various absorber temperatures. The absorber tube is coated with a black chrome selective surface, and the emissivity is taken as 0.2 (Chromasun, Inc.). The cover glass at the top and sides of the cavity are modelled as convection boundaries with external heat loss coefficients of 15 W/m^2K, exchanging heat with an ambient temperature of 23^oC. The glass has an internal emissivity of 0.9. The base of the cavity and aluminium side walls are also modelled as convection boundaries with external heat loss coefficients of 5 W/m^2K, exchanging heat with an ambient temperature of 23^oC. The air flow in the cavity is modelled as laminar as the Rayleigh number is in the range of 1.8×10^4 - 2.7×10^7. Radiation is modelled using the Monte Carlo simulation method (Wang et al. 2010). All discretization is carried out using second order schemes and air properties are calculated using an ideal gas model. Minimum convergence criteria were set at 10^{-3} for

continuity and velocity, and 10^{-6} for energy. A hybrid mesh is used with structured quadrilateral elements in the wall zones and unstructured triangular elements in the central zone of the collector cavity. The resulting mesh size is approximately 3 mm, with 60,000 mesh points in total. A grid dependency study has been undertaken to ensure the adequacy of this mesh density.

5. Experiment

An electrically heated absorber tube has been constructed to allow direct measurement of losses under laboratory conditions. A schematic representation of the equipment used to supply electrical power to the heating elements inside the absorber tubes is illustrated in Fig. 5. The absorber tube surface temperature is a function of the ambient temperature, thermal resistance from tube surface to the ambient environment and the heat lost. Under steady-state temperatures, all the electrical power applied to the heating element is lost through convection and radiation heat transfer into the cavity heat. The overall heat loss coefficient (U) of the absorber tube can be calculated by:

$$U = \frac{P}{A_{abs}\,(T_{abs} - T_a)} \qquad \text{(eq. 1)}$$

Where, P is the electric power supplied to the heating element, A_{abs} is the absorber tube surface area, T_{abs} is the absorber tube average surface temperature and T_a is the ambient temperature.

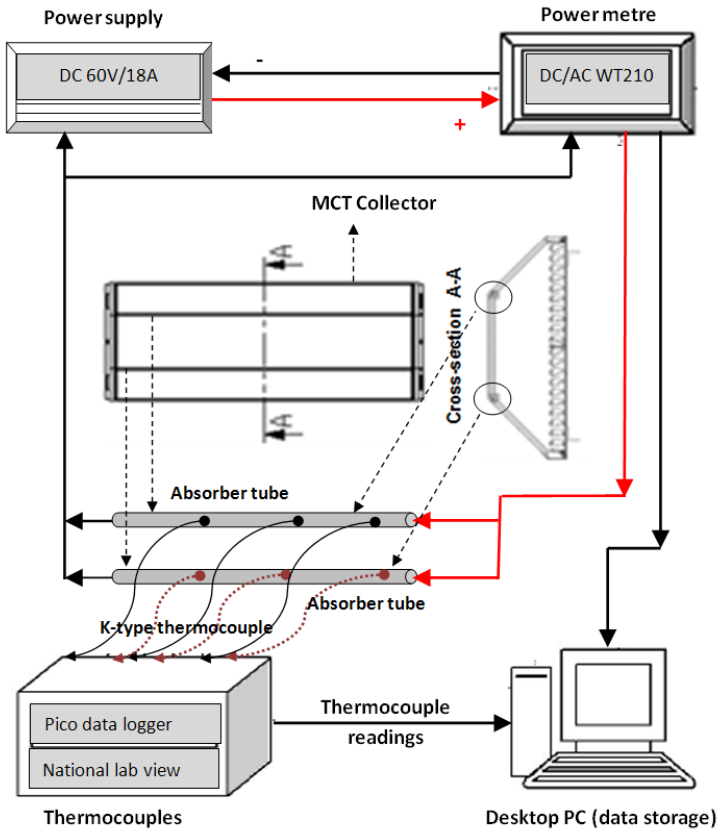

Fig. 5: Schematic diagram of the experimental setup

K-type fibreglass insulated thermocouples were used to measure the absorber tube temperatures inside the collector. The temperature measurement system was calibrated against a standard platinum resistance thermometer. Measurements from the thermocouples and power supply are recorded on a laptop PC. During operation, a time interval of approximately one hour is required for the system to reach steady state (Fig.6).

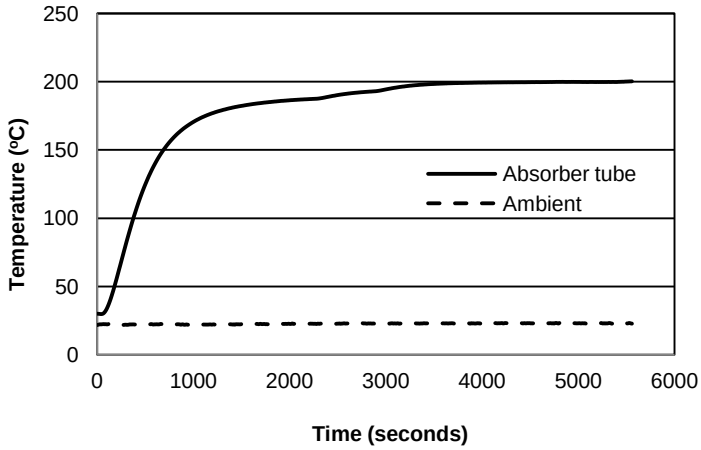

Fig. 6: Time required to reach steady-state condition (P_{abs} = 295 watt, T_a = 23°C)

The emissivity of the absorber tube was measured using an infrared camera (FLIR-TITANIUM 560M). Infrared calibration was performed by comparing IR and thermocouple measurements of the heated tube. Fig.7 shows an infrared photograph of the absorber tube. The average temperature measured by the thermocouples attached to the tube was 200°C. To match this temperature with the infrared measurements, the emissivity of the absorber tube (ε_{abs}) was set at 0.6 using the camera settings. However, using manufactures data (Lowery, 1981) the calculated equivalent emissivity of the absorber tube at 200°C was 0.24 (Fig.8). One possible reason for the difference is that while modifying the tube and attaching/reattaching the thermocouples numerous times, the selective surface may have been damaged.

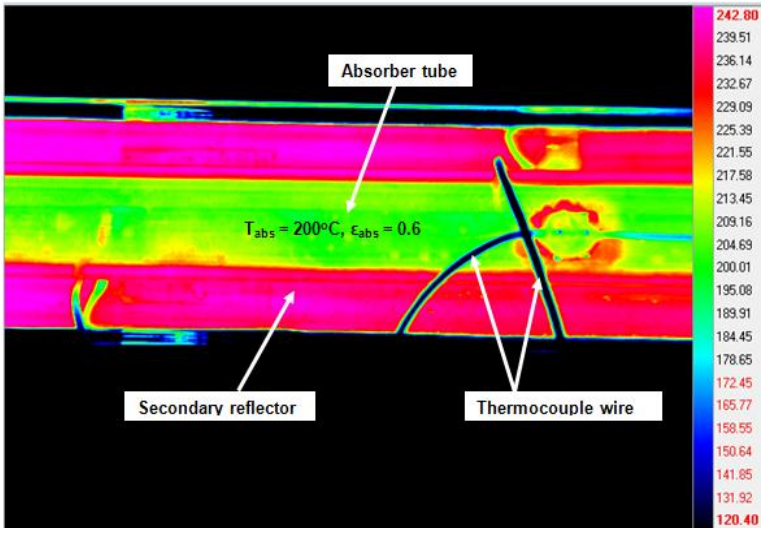

Fig. 7: Infrared photograph of absorber tube from bottom view (T_{abs} = 200°C, ε_{abs} = 0.6, Infrared wavelength = 3-5µm)

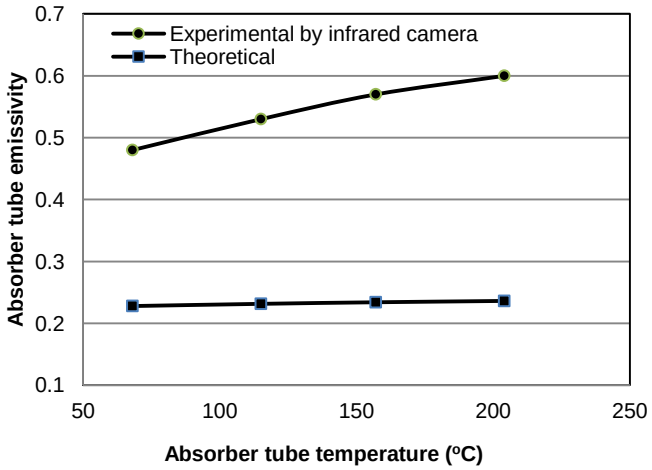

Fig. 8: Absorber tube emissivity for different absorber temperatures

Flow visualisation experiments were also performed to test the validity of the numerical model. The experimental set-up used a Nd:YAG continuous laser and digital camera. A modified MCT collector was used to facilitate optical access for the laser light and camera. The base was replaced by a plastic cover (without mirrors) and a viewing hole was made on the front face of the collector.

6. Results

6.1 Experimental results

Fig. 9 shows the heat loss measurements as a function of absorber tube temperatures. The measurements show that the tube reaches a temperature of approximately 200°C when 295W of energy is applied to each of the absorber tubes.

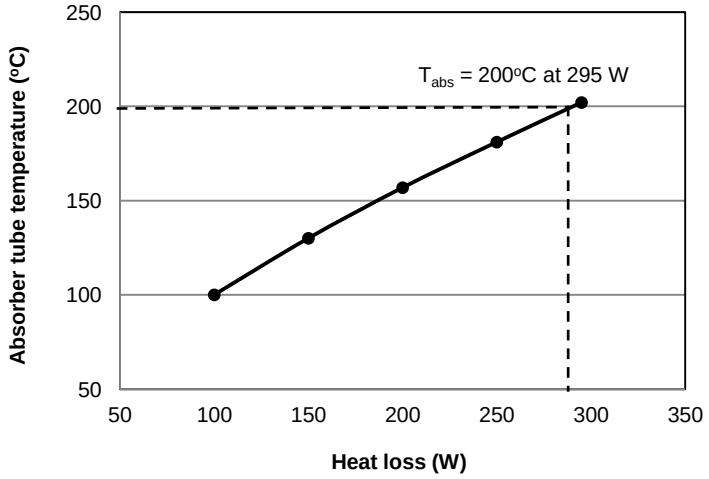

Fig. 9: Experimental heat loss vs. temperature for an absorber tube

The effect of inclining the MCT collector was also investigated over an inclination range of 0° to 20°. Fig. 10 illustrates that there is negligible effect of inclination up to 20°.

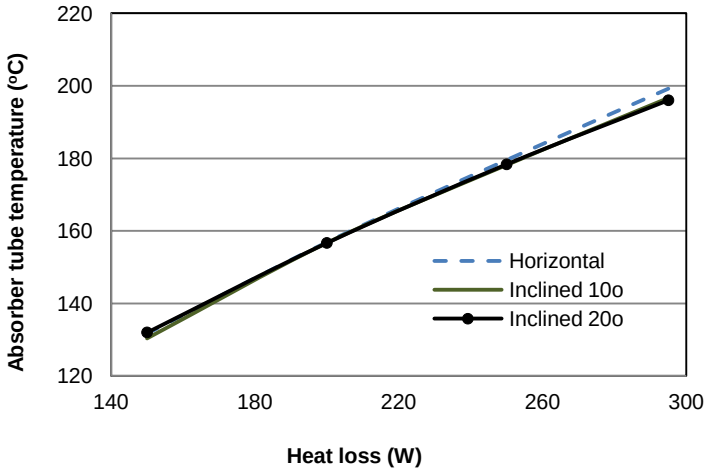

Fig. 10: Experimentally measured temperature as a function of input power

6.2 CFD results

The air flow patterns in the receiver cavity of the collector are shown in Fig. 11. Locations where fluid motion is fastest are along the glass side walls, and along the top surface. The next fastest fluid motion is a layer along the upper glass cover, with the fluid dropping down into the cavity from the top glass boundary at the symmetry plane. Although the bottom convective cells cover most of the cavity they do not significantly affect convection around the absorber. Rising fluid around the absorber tube is entrapped by the secondary reflector thus reducing the convective heat loss from the absorber tube to the cavity (Fig. 12). In this study the secondary reflector around the absorber tube was considered to be a thin aluminium sheet. It may be possible to reduce the strength of the upper convection cell by using an insulated reflector. For the boundary conditions specified in the CFD simulations, the results show significant thermal gradients in the cavity only around the absorber and secondary reflector (Fig. 13).

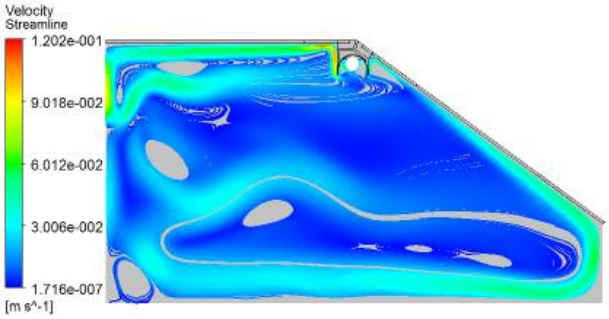

Fig. 11: Velocity streamlines in the cavity receiver (absorber tube temperature 200°C)

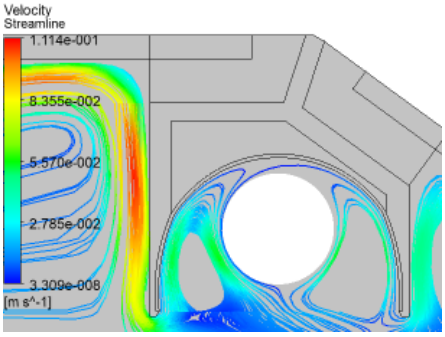

Fig. 12: Streamlines near the receiver section (absorber tube temperature 200°C)

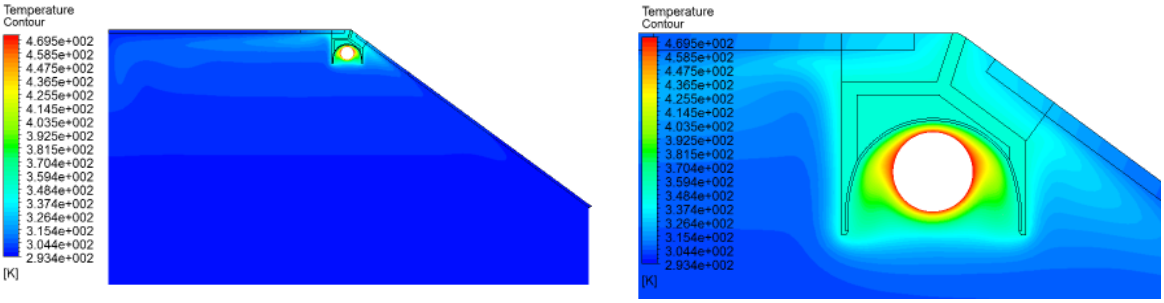

Fig. 13: (a) Temperature contours, (a) in the cavity receiver, (b) near the receiver (absorber tube temperature 200°C)

Due to the mixing caused by the bottom convection cell there is a relatively constant temperature in the cavity below the level of the absorber tube and a higher temperature convection cell under the top glass surface as shown in Figs. 14 & 15.

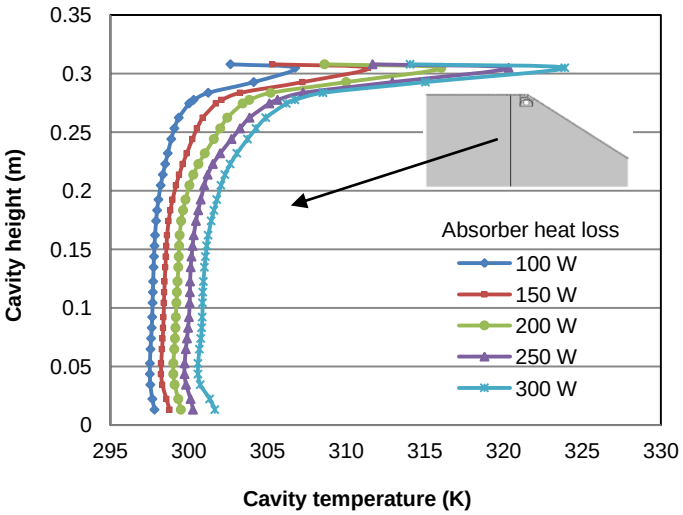

Fig. 14: Temperature profiles within the cavity for different absorber heat loss

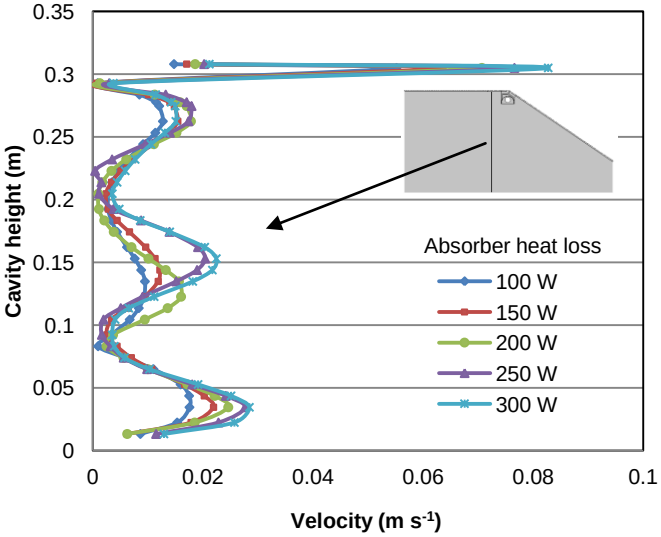

Fig. 15: Velocity profiles within the cavity for different absorber heat loss

Due to the low emissivity of the absorber selective coating the radiation heat loss is only 15% to 20% of the convective heat loss (Fig. 16). The CFD model indicates that the total heat loss at 200°C is approximately 77W per metre length compared to an expected solar input of approximately 300W to 400W per meter length. Heat loss from different boundary zones is shown in Fig. 17.

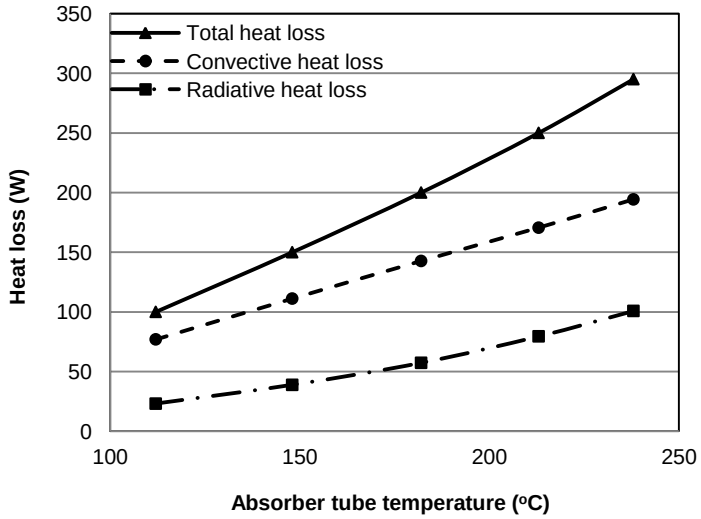

Fig. 16: Absorber heat loss for different absorber temperatures

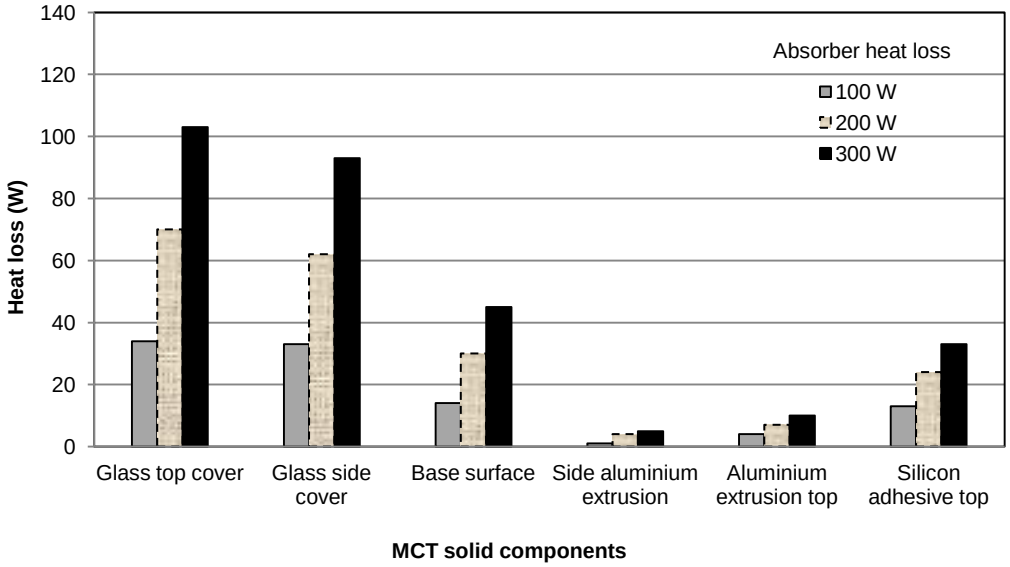

Fig. 17: Heat loss of external boundary elements for different absorber heat loss

6.3 Comparison between Experimental and CFD results

The heat loss predicted by the CFD model (230W) under –predicts the experimental results (295W) at 200°C absorber temperature by approximately 22% (Fig. 18). There are a number of uncertainties in the experimental work, the main ones being the emissivity measurements. The infrared testing indicated that the emissivity of the absorber tube used in this experiment was 0.6 at 200°C. However, the CFD model used an emissivity of only 0.2, which could explain some of the differences. Minimising radiation heat loss results successful modelling of the cavity and therefore the accuracy of the absorber tube emissivity reading is important. Fig.19 shows the absorber tube temperature decreases as absorber emissivity increases. A second area of uncertainty is the determination of the appropriate convection coefficient to be applied to the base cover and side covers of the cavity model. A three-dimensional CFD model is also being developed to more accurately represent the collector heat losses through the side cover walls.

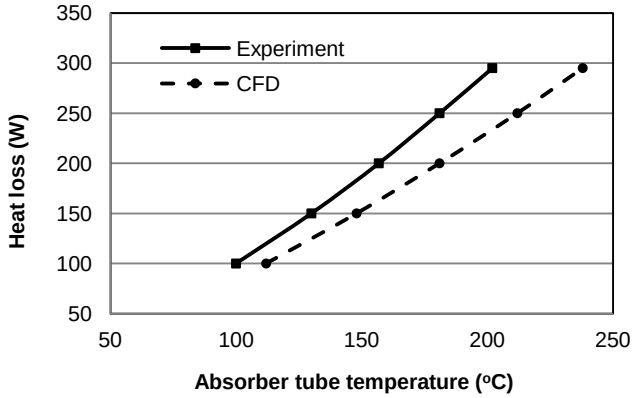

Fig. 18: Heat loss comparison of CFD model and experiment

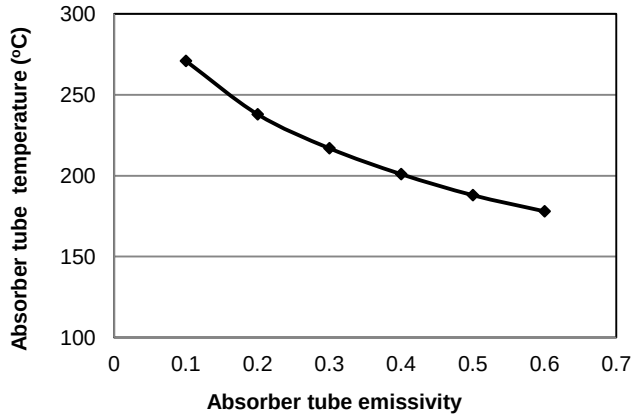

Fig. 19: Absorber tube temperatures versus absorber emissivity for 295 watt heat loss (CFD model)

The overall heat loss coefficient of the absorber tube at 200°C from CFD results is approximately 9 W/m^2/K, whereas the experimentally measured overall heat loss coefficient is approximately 11 W/m^2/K. Correlations between the overall heat loss coefficient and the absorber temperature were developed and shown in Fig. 20. The general relationship between overall heat loss coefficient *(U)* and absorber tube temperature *(T_{abs})* can be given as follows (Singh et.al. 2010).

$$U = a \,.\, (T_{abs})^b \qquad \text{(eq. 2)}$$

Where *a* and index *b* are constant for $50^oC \leq T_{abs} \leq 250^oC$.

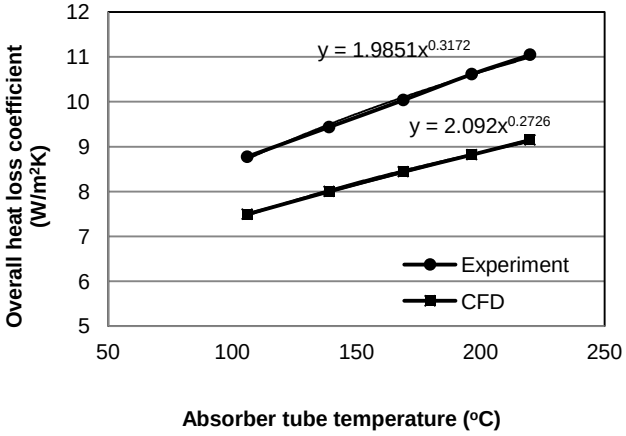

Fig. 20: Variation of overall heat loss coefficient vs. absorber tube temperature for CFD model and experiment

Figs. 21-22 shows a comparison of the CFD velocity flow fields and experimental results. The photograph assists in validating the CFD model, as the flow visualisation clearly captures the airflow rising around the secondary reflector, as predicted by CFD simulation. There are common traits of convection cells within the cavity of the collector.

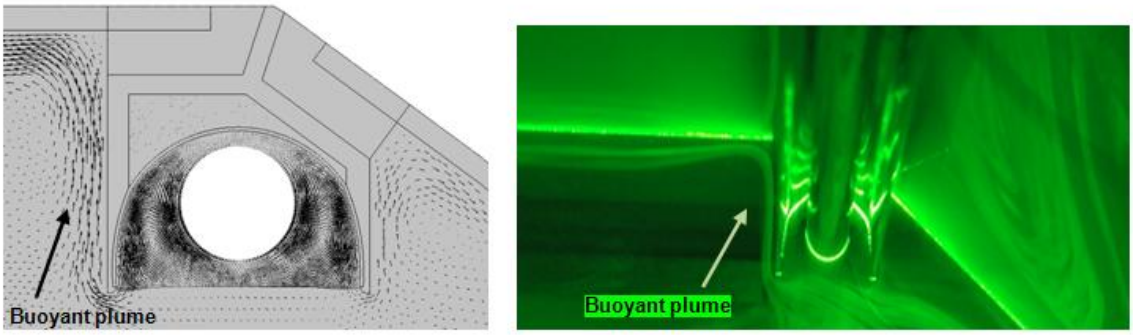

(a) (b)

Fig. 21: Airflow near the absorber tube, (a) CFD, (b) Flow visualisation

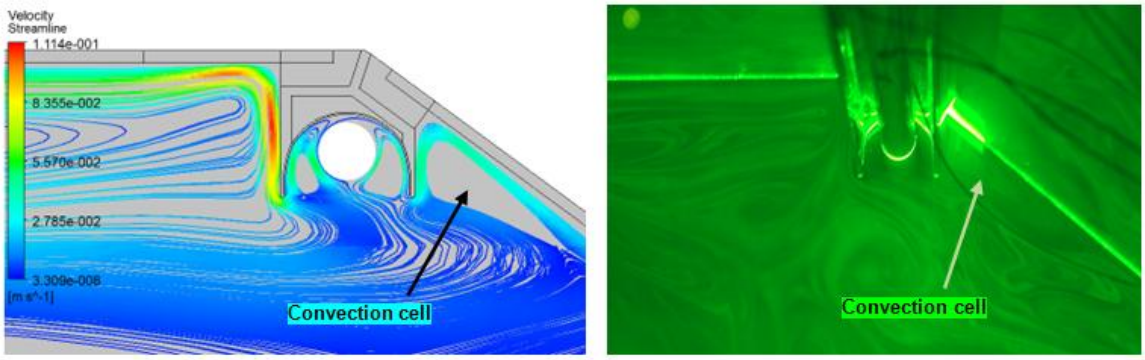

(a) (b)

Fig. 22: Airflow in the receiver cavity, (a) CFD, (b) Flow visualisation

The MCT thermal efficiency characteristic was determined by combining the calculated optical efficiency (Sultana et al., 2011) and heat loss as plotted in Fig. 23. Solar beam radiation is taken as G = 1000 W/m^2. The MCT system shows an efficiency of 56% at its design operating temperature of 200^{o}C.

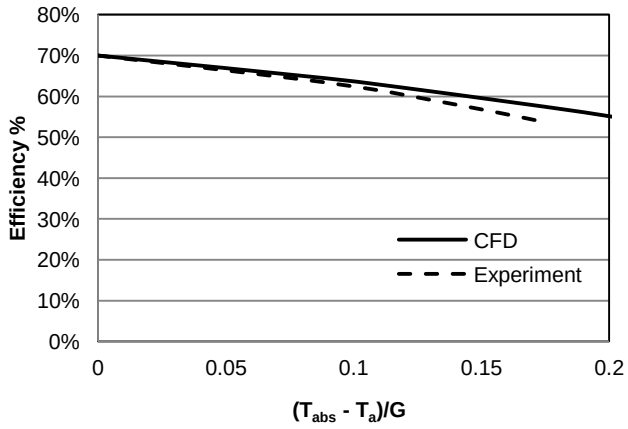

Fig. 23: MCT collector efficiency

7. Conclusion

Preliminary results have been obtained for the performance of a new cavity solar collector incorporating a linear Fresnel micro-concentrator. The performance was numerically simulated using computational fluid dynamics package, ANSYS-CFX. To analyse the thermal performance of the collector, a 2-D numerical simulation of convective and radiation heat loss has been carried out for steady-state laminar conditions and total heat loss coefficient obtained. Natural convection inside the cavity and thermal radiation between surfaces were modelled. Experiments performed to determine the heat lost from the MCT collector for varying operating temperatures. In comparison to the CFD model, the experimental results indicated 22% higher heat loss. Infrared testing revealed the selective surface of the absorber tubes is 0.6 which is higher than the design value of 0.2 used for CFD study. However, another possibility is that the heat transfer coefficient assumptions in CFD were understated. Experimental flow visualisation of air movement inside the collector yielded very similar results to the CFD velocity vectors, providing some confidence for numerical model. The work presented here indicates that the MCT collector has an efficiency of about 56% at its design operating temperature of 200^{o}C.

Acknowledgments

The present work is supported by Chromasun Inc., San Jose, CA 95112, USA. The authors would like to thank Mikal Greaves and Andrew Tanner for their support and assistance during the course of this project.

8. References

1. ANSYS CFX Help Manual 12.1, www.ansys.com.
2. Chromasun, Inc., San Jose, CA 95112, USA, www.chromasun.com.
3. Gee, R., Cohen, G., Greenwood, K., 2003. Operation and preliminary performance of the Duke Solar Power Roof: A Roof-integrated solar cooling and heating system. Duke Solar Energy, LLC, 2101, Westinghouse Boulevard, Raleigh, NC 27604. International Solar Energy Conference. p 295-300.
4. Juanico, L., 2008. A New design of roof-integrated water solar collector for domestic heating and cooling, Journal of Solar Energy, 82, pp. 481-492.
5. Lowery, J.R., 1981. Solar energy absorption characteristics and the effects of heat on the optical properties of the several coatings. NASA Thechnical memorandum, NASA-TM-82414.
6. Petrakis, M., Narakos, G., Kaplanis, S., 2009. Roof integrated mini-parabolic solar collectors. Comparison between simulation and experimental results. Open Fuels and Energy Science Journal. 2, 71-81.
7. Reynolds, D.J., Jance, M.J., Behnia, M., Morrison, G.L., 2004. An experimental and computational study of the heat loss characteristics of a trapezoidal cavity absorber. Journal of Solar Energy. 76, 229-234.
8. Singh, P.L., Sarviya, R.M., Bhagoria, J.L., 2010. Heat loss study of trapezoidal cavity absorbers for linear solar concentrating collector. Energy Conversion and Management, 51, 329-337.
9. Sultana, T., Bhardwaj, Morrison, G.L, Rosengarten, G., 2011. Heat Loss characteristics of a roof integrated solar micro-concentrating collector, ASME 5th International conference on Energy Sustainability. Washington DC, USA.
10. Sultana, T., Morrison, G.L, Tanner, A., Greaves, M., Lievre, P.L., Rosengarten, G., 2010. Heat Loss from Cavity Receiver for Solar Micro-Concentrating Collector. AuSES Solar Conference. Canberra, Australia.
11. Wang, Y., Dong, X., Wei, J.H., 2010. Numerical simulation of the heat flux distribution in a solar cavity receiver. Journal of Frontiers of energy and power engineering in China,Research article. 1673-7393 (print).